Minimax Theory and its Applications

Volume 11 (2026), No. 3s, 400 to 408

A Hybrid Optimization Framework Based on a Lightweight Dual-Branch Swin Transformer for Early Lung Cancer Detection and Classification

Benoy Abraham[1], R. S. Vinod Kumar[2], S S Kumar[3], Shahi .D[4]

[1]Ph.DResearch Scholar, Department of Electronics and Communication Engineering, Noorul Islam Centre for Higher Education, Kumaracoil, Tamil Nadu, India
[2,4]Professor, Assistant Professor, Department of Electronics and Communication Engineering, Noorul Islam Centre for Higher Education, Kumaracoil, Tamil Nadu, India
[3]Associate Professor, Department of Electronics and Instrumentation Engineering, Noorul Islam Centre for Higher Education, Kumaracoil, Tamil Nadu, India
Email: benoyab@fisat.ac.in, rsvinodkumar69@yahoo.co.in, kumarss@live.com, shahijulian@gmail.com

Abstract
Lung cancer arises from the uncontrolled growth of cells within lung tissues, posing a significant threat to respiratory functions crucial for oxygenation and carbon dioxide elimination in the human body. Early detection of malignant cells in the lungs is paramount, yet challenging due to the asymptomatic nature of early-stage lung cancer. Existing deep learning-based models for lung cancer detection require computational resources, presenting implementation challenges for healthcare centers. Thus, there is an urgent need for a sensitive and accurate approach to early lung cancer diagnosis. In this study, we propose an innovative approach to early lung cancer detection and classification, leveraging a hybrid process that integrates optimal segmentation, feature extraction, feature selection, and classification techniques. Our methodology combines the modified pity beetle optimization (MPBO) algorithm for optimal segmentation of CT scan and X-ray images, followed by feature extraction and optimization using DefenseNet with normative fish swarm optimization (NFSO) algorithm. Furthermore, we utilize lightweight dual-branch Swin transformer (LDB-ST) for early detection and classification of lung cancer subtypes, including adenocarcinoma, large cell carcinoma, and squamous cell carcinoma, in addition to identifying healthy lung tissue. We evaluate the performance of our model using benchmark datasets such as Chest CT Scans, LIDC-IDRI, and LUNA16. Comparative analysis with existing models demonstrates the superior performance of the proposed approach, with the LDB-ST model achieving a significant improvement of 5.801% in accuracy and 6.061% in F-measure. These findings highlight the potential of the proposed methodology to revolutionize early lung cancer diagnosis, offering enhanced accuracy and efficiency in clinical settings.

Keywords: Lung cancer, Early detection, Classification, Swin transformer, optimal segmentation

1. Introduction

One of the most prevalent and deadly malignancies, lung tumors puts a strain on our medical facilities and society as a whole [1]. Along with 1.8 million fatalities, over two million cases annually make it the most common cancer in the world. The primary kinds of lung cancer, non-small cell lung cancer (NSCLS) and small cell lung cancer (SCLC) are characterized by different molecular and histological features. The majority of lung cancer instances consist of recurrent carcinoma of squamous cells, giant cell tumors, and adenoma [2]. Early identification, therapy, and smoking cessation have improved lung cancer prognoses, but the five-year survival rate is still 19% [3]. Lung cancer also disproportionately affects underserved and marginalized communities due to healthcare access inequities [4]. Traditional lung cancer classification systems have helped diagnose and characterize cancers, but they have limitations. Histopathological analysis' subjectivity and interobserver variability are drawbacks. Pathologists' interpretation of tissue specimens depends on experience, training, and judgment, resulting in tumor categorization and sub-type errors [5].

Transformer-based topologies have revolutionized neural network processing in machine learning. Transformers, originally designed for natural language processing, have excelled in computer vision, medical picture analysis, and more [6]. Transformer topologies like Swin transformer and data-efficient picture transformer (DeiT) excel at picture categorization and other computer vision applications. The hierarchical

architecture with shifting windows of Swin transformer efficiently captures global and local visual information [7]. Transformer based models can capture fine-grained spatial dependencies, incorporate multi-modal information, and adapt to different imaging procedures and anatomical differences for medical image processing [8].

1.1 State of art works on lung cancer detection and classification

A few works done in this category are listed in this section. They are Raza et al. 2023 [9] investigated computational methods including algorithms for DL and ML to expand CT lung tumor discovery speed and correctness. Lung-EffNet is fabricated on EfficientNet, a popular DL network, with classification head changes. Pandit et al. 2023 [10] suggested a solution using an autoencoder system to improve accuracy, multi space pictures in CNN pooling layers, and the Adam Algorithm for refinement to overcome these issues and the accuracy rise from 98.9% to 99.5% and a handling time decrease from 10 frames per second to 12 seconds. Dwivedi et al. 2023 [11] presented an original understandable artificial intelligence (XAI)-related DL system to find a compact collection of biomarkers for NSCLC, especially its two major subtypes, LUAD and LUSC. Naseer et al. 2023 [12] suggested a method, with multiple steps. An altered U-Net design is used for lobe separation. To further sort the collected nodules into malignant and non-cancerous groups, support vector machine and an altered AlexNet model are used. The improved AlexNet-SVM classification model produces remarkable results, such as 97.98% accuracy, 98.84% sensitivity, 97.47% specificity, a 97.53% precision, and a 97.70% F1 score.

Siddiqui et al. 2023 [13] suggested an approach which combines many methods for classification, with SVM producing optimal recital strictures, by utilizing Gabor filters and an enhanced deep belief network (E-DBN) with flowed RBMs. AR et al. 2023 [14] suggested using machine learning and pattern recognition to classify lung tumor from CT images. LCD-CapsNet, a unique deep learning framework, blends a CNN with a CapsNet to handle large data volumes and achieve spatial invariance needed for lung tumor finding and categorization. The performance of LCD-CapsNet surpasses that of CapsNet in the finding and cataloging of lung tumor. Prakash et al. 2023 [15] presented the development of the enhanced Elman spike neural network customized with the flamingo search optimization procedure for the purpose of classifying lung tumor from CT images (EESNN-FSOA-LCC) which achieves 38.58%, 25.69%, and 43.87% higher accuracies, respectively. Sun et al. 2023 [16] examined the use of transformer models, notably the Swin Transformer, in artificial intelligence for lung cancer identification and segmentation. The pre-trained Swin-B model outperformed ViT by 2.529% in classification with 82.26% accuracy. Sun et al. 2024 [17] used self-learning weight aggregation to reduce semantic bias from WSI's many attributes. They used random patch training to extract vectors of attributes randomly from WSI to enrich model learning.

The remainder of this paper is organized as follows. Section 2 describes the proposed methodology using Lightweight Dual-Branch Swin Transformer architecture. Section 3 presents the experimental setup, comparative analysis, and discussion of the results. Finally, Section 4 concludes the paper by summarizing the key findings and directions for future research.

2. Methodology

We frame the orderly methodology utilized for the early discovery and characterization of cellular breakdown in the lungs utilizing a half and half structure coordinating ideal division, highlight extraction, include enhancement, and grouping procedures, alongside transformer-based engineering. Preprocessing of the CT scan images is essential to remove noise and artifacts that may affect the accuracy. The modified pity beetle optimization (MPBO) algorithm for optimal segmentation enables the precise delineation of the ROI corresponding to potential cancerous lesions within the lung images. Accurate segmentation is vital for isolating and focusing on areas indicative of lung cancer, facilitating subsequent analysis and classification tasks. Utilizing the DefenseNet architecture for feature extraction allows for the extraction of a comprehensive set of features from the segmented lung images. These features encompass deep features capturing intricate patterns, texture features highlighting textural properties, semantic features encoding high-level semantics, and statistical features characterizing the statistical distribution of pixel intensities. The normative fish swarm optimization (NFSO) algorithm is employed for feature optimization, selecting the most informative subset of features from the extracted feature pool. The lightweight dual-branch Swin transformer (LDB-ST) architecture serves as the classification model for distinguishing between different lung cancer subtypes and normal lung tissue. Utilizing the learned highlights and examples, LDB-ST orders the fragmented lung pictures into four classes, including Adenocarcinoma, Huge cell carcinoma, Squamous-cell carcinoma, and typical tissue.

2.1. Optimal Segmentation

In clinical imaging, for example, CT outputs and X-beam pictures, division is regularly used to distinguish and outline different physical designs or regions of interest within the images. The modified pity beetle optimization (MPBO) algorithm is a metaheuristic optimization algorithm inspired by the foraging behavior of pity beetles. It is problem-solving techniques that are inspired by natural phenomena or processes. They are utilized to find surmised answers for streamlining and search issues where it is computationally infeasible to track down an accurate arrangement. The underlying populace of forerunner particles is characterized as in Eqn. (1)

$$q^{(0)} = \left[q_1^{(0)}, q_2^{(0)}, ..., q_{B_{pop}}^{(0)}\right]^S \tag{1}$$

It $q_g^{(0)}$ addresses the ideal position vector or transfer hub area and is haphazardly situated in the C-layered search space as in Eqn. (2)

$$q_g^{(0)} = rst\left(B_{pop}, C, L, U\right) \tag{2}$$

Algorithm 1 describes the optimal segmentation using MPBO.

Algorithm 1 Optimal segmentation using MPBO

Input : Number of images, target images, maximum iteration
Output : ROI segmentation

1. Initialize the random population
2. Define initial population of precursor particles
   $q^{(0)} = \left[q_1^{(0)}, q_2^{(0)}, ..., q_{B_{pop}}^{(0)}\right]^S$
3. If i=0 , j=1
4. While Do
5. $$f_g(s) = \max\begin{cases} of_1 \\ of_2 \\ of_3 \end{cases}$$
   Compute the eligibility of each solution
6. Find the best attracts and seeks the newest people
   $$q_{birth,h}^{(j+1)} = \begin{cases} q_{birth,h}^{(j)}, & if\ f\left(q_{birth,h}^{(j)}\right) < \left(q_{g,K}^{(j)}\right) \forall g = 1,2,....B_{pop}, K = 1,2,....B_{broods} \\ q_{g,K}^{(j)}, & otherwise \end{cases}$$
7. The progenitor particles were randomly arranged on this now turbulent hunting ground.
   $$q_{g,K}^{(j)} = rst\left(B_{pop}, C, \left[q_{birth,h}^{(j)} * (1 - F_{Lt}), q_{borth,h}^{(j)} * (1 + F_{Lt})\right]\right)$$
8. The probe region by RST methods: $q_g^{(j)} = rst\left(B_{pop}, C, L^{(j)}, U^{(j)}\right)$
9. End if
10. Update the final value
11. End

2.2. Feature Extraction and Optimization

Feature extraction is process to extracts relevant information or characteristics, known as features, are extracted from raw data, such as images or signals. DefenseNet is DL architecture used for feature extraction tasks. DefenseNet, when applied to CT images, serves as a robust tool for extracting essential features crucial for medical image analysis. Through its convolutional layers, DefenseNet adeptly captures intricate texture details inherent in CT scans. Normative fish swarm optimization (NFSO) is an algorithm inspired by the collective behavior of fish swarms. To adjust the contention between the inquiry and abuse processes, the normative fish swarm algorithm (NFSA) is used to conduct a thorough global and local search for achieving an efficient global optimum with improved convergence speed. The algorithm for Feature Optimization Using the Novel Feature Selection Optimization (NFSO) is given in Algorithm 2

Algorithm 2 Feature Optimization Using the Novel Feature Selection Optimization (NFSO) Algorithm Technique

Input : Number of features, maximum iteration and termination condition
Output : Optimal best features

```
Set Up Parameters;
Random Fish Population Initialization, AF _INIT
WHILE
Determine Fitness of AFs' Current Position;
DO AF_FOLLOW
IF (AF_FOLLOW Fail) THEN
DO AF_PREY
IF (AF_PREY Fail) THEN
DO AF_RANDOM
End
Output P1;
DO AF_SWARM
END
Output P2;
   DO AF_NORM_COMM
END
Greedy Assortment from P1, P2;
NumFish+1;
END FOR
Update Best Fitness
END
Improved Adapt
End while
```

2.3. Lung Cancer Detection and Classification

Cellular breakdown in the lungs recognition and arrangement include the recognizable proof and order of cellular breakdown in the lung's subtypes, as well as recognizing solid lung tissue from harmful sores. This interaction is urgent for early conclusion, therapy arranging, and checking of cellular breakdown in the lung's patients. The lightweight dual-branch Swin transformer (LDB-ST) is DL architecture designed for this task. It combines elements of the Swin Transformer architecture, known for its effectiveness in processing images at multiple scales, with a lightweight design to facilitate efficient computation and deployment. Then, Convolutional Multilayer Perceptron (Conv-MLP) is integrated into each period of the Long Short-Term Memory Data Block (LDB-ST). This enhances the model's ability to detect long-range patterns by facilitating the connection of the Vision Transformer (ViT) with window associations.

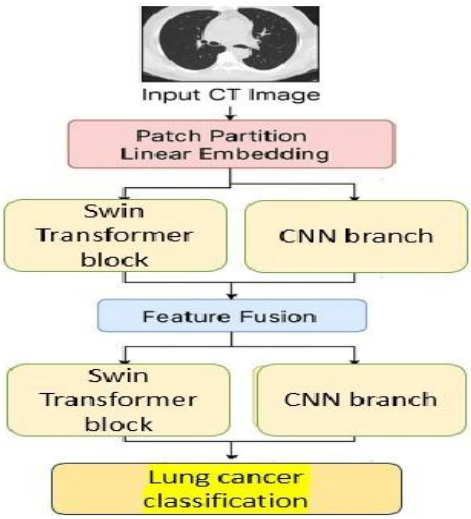


Fig 4: Block Diagram representation of the proposed LDB-ST model

At long last, the implanting vector arrangement is taken care of into the four flowed phases of the LDB-ST, and the result aspects down sampled at each stage are $x_1^{k-1} = Conv_{1\times1}\left(x^{k-1}\right)$ and H 8n × W 8n × 8C. For straightforwardness, expect that the contribution for a specific phase of the various leveled LDB-ST technique is $x_1^{k-1} = Conv_{1\times1}\left(x^{k-1}\right)$ the double branch design of LDB-ST parts it into $x_1^{k-1} = Conv_{1\times1}\left(x^{k-1}\right)$ segment by a 1 × 1 convolutional layer. For $x_1^{k-1} = Conv_{1\times1}\left(x^{k-1}\right)$, the window segregating approach is taken on to choose the result of l_layer in the transformer encoder.

Concerning the result, the CNN branch at first applies a 3 × 3 convolutional layer to separate highlights. Then, max pooling is embraced to significant solid areas for hold and rates up the model association, finally come by the result x_2^{k+1} as in Eqn. (3).

$$x_2^{k+1} = Maxpool\left(conv_{3\times3}\left(x_2^{k-1}\right)\right). \tag{3}$$

At last, the result x_2^{k+1} of the double branch LDB-ST module is gained by stacking and in the channel viewpoint and this can be framed as in Eqn. (4).

$$x^{k+1} = Concat\left(x_1^{k+1}, z_2^{k+1}\right). \tag{4}$$

In synopsis, the twofold branch module first packages the data highlight into two portions according to the channel viewpoint, the obligation is moved to the ViT part of the organized Conv_MLP to upgrade the associations among neighboring windows and work on the model's capacity to decipher by and large information.

3. Experimental Results and Discussion

The performance of the proposed LDB-ST model is validated using well-known benchmark datasets including Chest CT Scans, LIDC-IDRI, and LUNA16 and their details are given in Table 2. All trials were conducted using an AMD Ryzen 7-5800HS processor with 40 GB of available memory, and simulations were performed using an NVIDIA GeForce RTX 4060 GPU. Additionally TensorFlow and Python are utilized to obtain all the results.

Table 2. Description of datasets

Description	Chest CT Scans	LIDC-IDRI	LUNA16
Number of images	1000	463	888
Size	125MB	4Gb	66GB
Type of image	CT scan	x-ray image	CT scan
Testing images	800	370	710
Training images	200	93	178

3.1 Experimental Results

The confusion matrix representing the performance of the model proposed is illustrated in Fig. 4. The three datasets namely, CT scan images, LIDC-IDRI, and LUNA16, along with their combined dataset were used to test the model. In all the datasets, the proposed LDB-ST model performed exceptionally well, with an accuracy of 99.52% on the combined dataset at 100 epochs. Fig. 7 depicts the Confusion Metrics for the proposed algorithms is shown in Fig. 7.

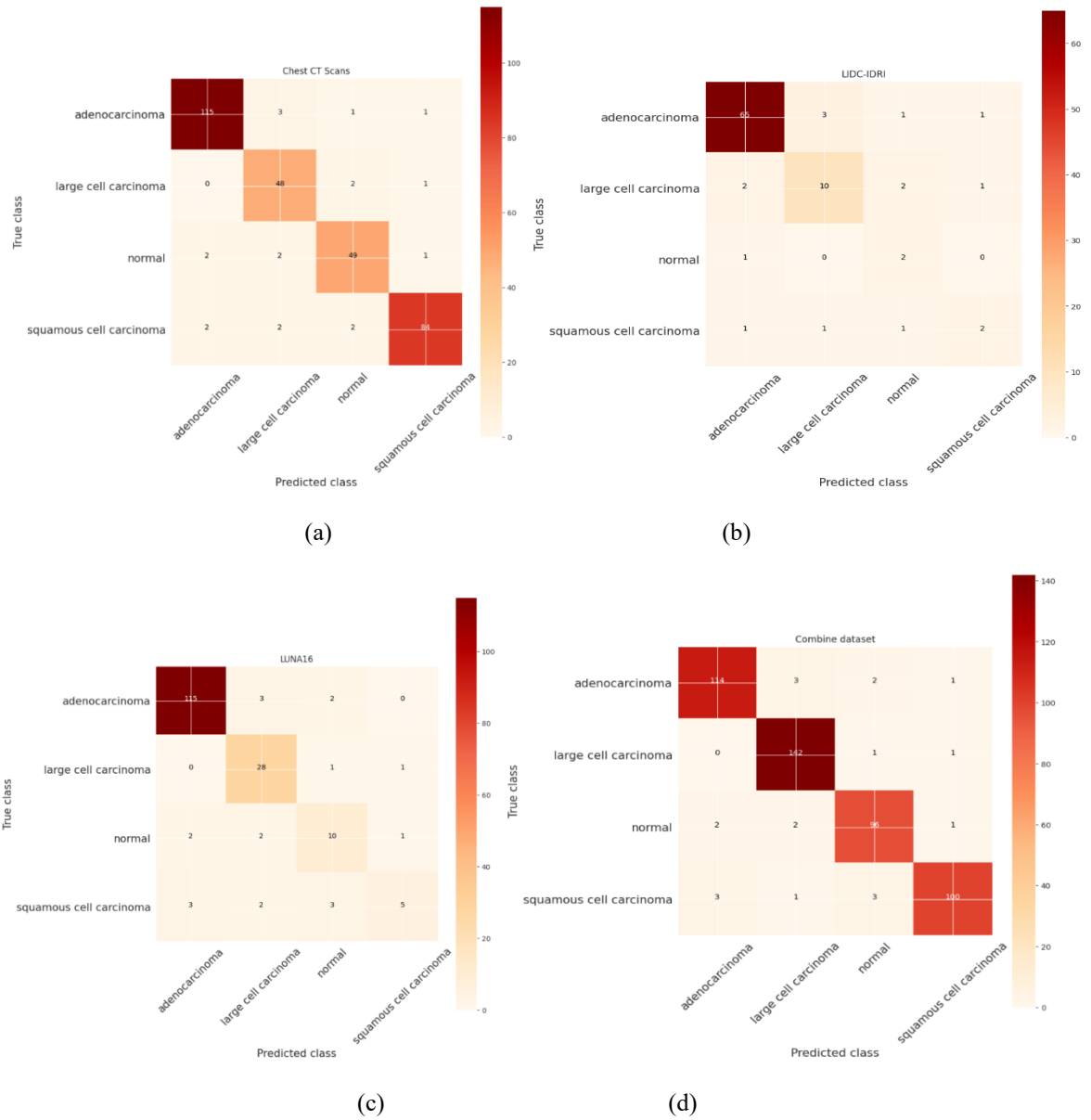


Fig 7: Confusion matrix of (a) using CT scan images (b) using LIDC-IDRI (c) using LUNA16 and (d) using combined dataset.

3.2 Comparative Analysis with the state of art works

Table 7 presents the results of proposed and existing state-of-the-art works for lung cancer detection and classification, evaluated in terms of accuracy, precision, recall, and F-measure. Let's analyze the findings with a focus on the percentage-wise increase or decrease compared to the XGBoost+RFA model. The XGBoost+RFA model serves as the baseline, achieving an accuracy of 84.013%. As we compare subsequent models, we observe substantial improvements across various metrics. For instance, the ANN model achieves an accuracy of 96.671%, marking a significant increase of approximately 12.658% from the baseline. Similarly, the CNN model demonstrates notable progress, achieving an accuracy of 93.549%, representing an increase of approximately 9.536%. Moving to precision, recall, and F-measure, we notice varying trends across models. The LP+ASR model achieves a high accuracy of 99.012%, with a precision of 89.025%, indicating a trade-off between accuracy and precision. For instance, SqueezeNet achieves an accuracy of 90.258%, with precision, recall, and F-measure values ranging from 89.289% to 89.927%, showcasing balanced performance. DenseNet, for example, attains an accuracy rate of 93.256% and showcases high precision, recall, and F-measure values, indicating strong performance in tasks related to detecting and classifying lung cancer. The LDB-ST model emerges as the top performer, achieving an accuracy of 99.522% and maintaining high precision, recall, and F-

measure values, highlighting its effectiveness in accurately detecting and classifying lung cancer subtypes. The results demonstrate significant improvements in accuracy, precision, recall, and F-measure across various state-of-the-art models compared to traditional methods. DL architectures, ATT-DenseNet and LDB-ST, exhibit superior performance, underscoring their potential in advancing lung cancer detection and classification tasks.

Table 7: Comparison of the proposed and State of Art approaches for Lung Cancer Detection and Classification

Models	**Values in %**			
	Accuracy	**Precision**	**Recall**	**F-measure**
XGBoost+RFA [18]	84.01	NA	NA	NA
ANN [19]	96.67	NA	NA	NA
Image processing [20]	72.25	NA	NA	NA
CNN [21]	93.54	95.71	NA	NA
LP+ASR [22]	99.01	89.02	NA	NA
Fused image [23]	99.00	NA	89.02	NA
SqueezeNet [24]	90.25	90.28	89.56	89.92
AlexNet	92.15	92.35	90.56	91.44
DenseNet	93.25	93.98	93.05	93.51
ATT-DenseNet	94.56	94.47	94.48	94.48
LDB-ST	**99.52**	**99.26**	**99.53**	**99.39**

4. Conclusion

A novel method for early detection and classification of lung cancer is introduced utilizing a hybrid process that integrates optimal segmentation, feature extraction, feature selection, and classification techniques. Our methodology leverages the modified pity beetle optimization (MPBO) algorithm for precise segmentation of CT scan and X-ray images, followed by feature extraction and optimization using DefenseNet coupled with the normative fish swarm optimization (NFSO) algorithm. Additionally, we utilized the lightweight dual-branch Swin transformer (LDB-ST) for detect and classify lung cancer subtypes, including adenocarcinoma, large cell carcinoma, squamous cell carcinoma, and identifying healthy lung tissue. Our model's performance is evaluated using benchmark datasets such as Chest CT Scans, LIDC-IDRI, and LUNA16. Our tests show that our proposed LDB-ST model achieves exceptional results with an accuracy of 99.522%, precision of 99.26%, recall of 99.539%, and F-measure of 99.399%. When compared to existing models, our approach stands out, with the LDB-ST model demonstrating a significant improvement of 5.801% in accuracy and 6.061% in F-measure. As a future work, the proposed LDB-ST model can be extended by integrating multi-scale feature fusion and self-supervised pretraining to further enhance classification performance and generalization on diverse datasets.

References

1. Lazam, N. M., Shair, S. N., Asmuni, N. H., Jamaludin, A., &Yusri, A. A. (2023, February). Forecasting the incidence rates of top three cancers in malaysia. In AIP Conference Proceedings (Vol. 2500, No. 1). AIP Publishing.

2. Li, F., Yang, Y., Xu, Y., Li, K., Song, L., Xue, Y., & Dong, D. (2023). Comparative study of the genomic landscape and tumor microenvironment among large cell carcinoma of the lung, large cell neuroendocrine of the lung, and small cell lung cancer. Medicine, 102(4), e32781.

3. Yang, C. Y., Lin, Y. T., Lin, L. J., Chang, Y. H., Chen, H. Y., Wang, Y. P., & Yang, P. C. (2023). Stage shift improves lung cancer survival: real-world evidence. Journal of Thoracic Oncology, 18(1), 47-56.

4. Wu, J. T. Y., Wakelee, H. A., & Han, S. S. (2023). Optimizing lung cancer screening with risk prediction: current challenges and the emerging role of biomarkers. Journal of Clinical Oncology, 41(27), 4341-4347.

5. Maleki, E. H., Bahrami, A. R., &Matin, M. M. (2024). Cancer cell cycle heterogeneity as a critical determinant of therapeutic resistance. Genes & diseases, 11(1), 189-204.

6. Gao, Q., Yang, L., Lu, M., Jin, R., Ye, H., & Ma, T. (2023). The artificial intelligence and machine learning in lung cancer immunotherapy. Journal of Hematology & Oncology, 16(1), 55.

7. Aalam, S. W., Ahanger, A. B., Masoodi, T. A., Bhat, A. A., Akil, A. S. A. S., Khan, M. A., & Bhat, M. R. (2024). Deep learning-based identification of esophageal cancer subtypes through analysis of high-resolution histopathology images. Frontiers in Molecular Biosciences, 11, 1346242.

8. Sivakumar, S., Moore, J. A., Montesion, M., Sharaf, R., Lin, D. I., Colón, C. I., & Lovly, C. M. (2023). Integrative analysis of a large real-world cohort of small cell lung cancer identifies distinct genetic subtypes and insights into histologic transformation. Cancer discovery, 13(7), 1572-1591.

9. Raza, R., Zulfiqar, F., Khan, M. O., Arif, M., Alvi, A., Iftikhar, M. A., &Alam, T. (2023). Lung-EffNet: Lung cancer classification using EfficientNet from CT-scan images. Engineering Applications of Artificial Intelligence, 126, 106902.

10. Pandit, B. R., Alsadoon, A., Prasad, P. W. C., Al Aloussi, S., Rashid, T. A., Alsadoon, O. H., &Jerew, O. D. (2023). Deep learning neural network for lung cancer classification: enhanced optimization function. Multimedia Tools and Applications, 82(5), 6605-6624.

11. Dwivedi, K., Rajpal, A., Rajpal, S., Agarwal, M., Kumar, V., & Kumar, N. (2023). An explainable AI-driven biomarker discovery framework for Non-Small Cell Lung Cancer classification. Computers in Biology and Medicine, 153, 106544.

12. Naseer, I., Akram, S., Masood, T., Rashid, M., &Jaffar, A. (2023). Lung cancer classification using modified U-Net based lobe segmentation and nodule detection. IEEE Access.

13. Siddiqui, E. A., Chaurasia, V., &Shandilya, M. (2023). Detection and classification of lung cancer computed tomography images using a novel improved deep belief network with Gabor filters. Chemometrics and Intelligent Laboratory Systems, 235, 104763.

14. AR, B., RS, V. K., & SS, K. (2023). LCD-capsule network for the detection and classification of lung cancer on computed tomography images. Multimedia Tools and Applications, 82(24), 37573-37592.

15. Prakash, T. S., Kumar, A. S., Durai, C. R. B., & Ashok, S. (2023). Enhanced Elman spike Neural network optimized with flamingo search optimization algorithm espoused lung cancer classification from CT images. Biomedical Signal Processing and Control, 84, 104948.

16. Sun, R., Pang, Y., & Li, W. (2023). Efficient lung cancer image classification and segmentation algorithm based on an improved swin transformer. Electronics, 12(4), 1024.

17. Sun, K., Zheng, Y., Yang, X., &Jia, W. (2024). A novel transformer-based aggregation model for predicting gene mutations in lung adenocarcinoma. Medical & Biological Engineering & Computing, 1-14.

18. Uddin, J., 2024. Attention-Based DenseNet for Lung Cancer Classification Using CT Scan and Histopathological Images. Designs, 8(2), p.27.

19. Habib, M.A., Zhou, H., Iturria-Rivera, P.E., Elsayed, M., Bavand, M., Gaigalas, R., Furr, S. and Erol-Kantarci, M., 2023, January. Traffic steering for 5G Multi-RAT deployments using deep reinforcement learning. In 2023 IEEE 20th Consumer Communications & Networking Conference (CCNC) (pp. 164-169). IEEE.

20. Tang, W., Sun, J., Wang, S. and Zhang, Y., 2023. Review of AlexNet for Medical Image Classification. arXiv preprint arXiv:2311.08655.

21. Zhong, Z., Zheng, M., Mai, H., Zhao, J. and Liu, X., 2020, November. Cancer image classification based on DenseNet model. In Journal of physics: conference series (Vol. 1651, No. 1, p. 012143). IOP Publishing.

22. Avanzo, M., Stancanello, J., Pirrone, G. and Sartor, G., 2020. Radiomics and deep learning in lung cancer. Strahlentherapie und Onkologie, 196, pp.879-887.

23. Coudray, N., Ocampo, P.S., Sakellaropoulos, T., Narula, N., Snuderl, M., Fenyö, D., Moreira, A.L., Razavian, N. and Tsirigos, A., 2018. Classification and mutation prediction from non–small cell lung cancer histopathology images using deep learning. Nature medicine, 24(10), pp.1559-1567.

24. Faisal, M.I., Bashir, S., Khan, Z.S. and Khan, F.H., 2018, December. An evaluation of machine learning classifiers and ensembles for early stage prediction of lung cancer. In 2018 3rd international conference on emerging trends in engineering, sciences and technology (ICEEST) (pp. 1-4). IEEE.

25. Sampath Emani. (2026). Design and Analysis of a Compact High-Voltage Insulation System for Reliable Power Transmission. *National Journal of Electrical Electronics and Automation Technologies* , *2*(4), 49-55.

26. Selamawit Tadesse. (2026). Robust PLC-Based Automation Framework for Multi-Stage Industrial Process Control. *National Journal of Electrical Electronics and Automation Technologies* , *2*(2), 35-44.